

Dynamics of pattern formation in bacterial swarms

Edward B. Steager, Chang-Beom Kim, and Min Jun Kim^{a)}

Department of Mechanical Engineering and Mechanics, Drexel University, 3141 Chestnut Street, Philadelphia, Pennsylvania 19104, USA

(Received 12 November 2007; accepted 6 June 2008; published online 10 July 2008)

To gain a more thorough understanding of the dynamics of swarming bacteria, a nonlabeled cell tracking algorithm was used to study the velocity field of flagellated bacteria, *Serratia marcescens*, swarming on a soft agar plate. The average velocities for local regions regularly arranged over the entire flow field were investigated. The velocity field of the bacteria typically featured the combination of curvilinear translation and vortex modes. They repeated these patterns for short periods of time, forming several groups and dissipating. To further investigate the flow patterns generated by the collective motion of the swarming bacteria, the velocity field on the swarm was spatially correlated. The highest velocities and correlation lengths have been found to occur in the region from 0.5 to 1 mm from the swarm edge, followed by a steady decline as distance from the edge increases, and a sudden decrease in motion typically occurs between 2 and 4 mm from the swarm edge. © 2008 American Institute of Physics. [DOI: 10.1063/1.2953245]

INTRODUCTION

Bacteria such as *Serratia marcescens* or *Escherichia coli* swim in liquid environments by rotating thin helical flagellar filaments.¹ Other types of locomotion in the form of surface translocation can be found on semisolid surfaces and are referred to as swarming or gliding.² It has been commonly believed that all their motions are powered by the reversible rotary motor embedded in the cell membrane.³ On soft agar surfaces, bacterial colonies have been observed to grow rapidly through a collective mechanism.⁴

Swarming is a crucial behavior of organisms which span their territories or population in an environment. Among them, bacterial swarming is a form of flagella-dependent surface motility. The flagellar motions driven by the bacterial rotary motor eventually result in the collective motion of the swarming bacteria. Swarming bacteria are hyperflagellated, elongated, and migrate cooperatively.² Characteristic dynamic patterns of whirls and jets have been observed both in swarming bacteria as well as in high-cell density swimming populations,⁵ and the interplay of the roles of sensory mechanisms and hydrodynamic interactions is widely researched.⁶ Although communication mechanisms between swarming *S. marcescens* are not fully understood, research suggests that pattern formation in the active swarm may be influenced largely by hydrodynamic interactions between densely packed cells. Large-scale dynamic coherence has been observed in swimming populations of *Bacillus subtilis*.⁷ This phenomenon of dynamic coherence has been confirmed by simulation by accounting for hydrodynamic interactions of suspensions of self-propelled particles at low Reynolds number.⁸ Results of bacteria swimming in thin fluid films also provide evidence for the pure hydrodynamic origin of collective swimming.⁹ Further experimental work with small copper rods reveals that inanimate objects exhibit swarmlike

formations due to nonspecific interactions.¹⁰ In fact, these rods do not demonstrate swarming behavior unless the ends are rounded, resembling the elongated bacillus shape of swarming bacteria. Analytical models of bacterial swarming also reveal that swimming and swarming formations may be a result of physical interactions between individual bacteria.^{11,12} This research lends credence to an effort to understand the larger scale dynamics of the swarm. That is, the study of swarming formations may reveal dynamics consistent with a collective effort to rapidly populate environments which may otherwise remain unpopulated.

Recently, associated with the function of the flagella, bacteria have been used as actuators in microscale engineered devices.^{13–16} Bacterial monolayers, referred to as bacterial carpets, were created on microstructures by using a blotting method,¹⁷ and the swarming pattern is directly reproduced on the bacterial carpet. Controlled manipulation may be exerted by exploiting the existing bacterial chemical sensory mechanisms.^{18,19} However, the swarm plate dynamics have not been well understood. In this study, we employ a nonlabeled cell tracking method to trace the bacterial swarming flow field without fluorescence labeling or microspheres as tracers. This research is intended to lend fundamental insight into ongoing bacterial actuation studies with the specific goal of understanding the large-scale collective dynamics of the swarm through a study of pattern formation.

METHODS

The bacteria *S. marcescens* (ATCC 274, American Type Culture Collection, Manassas, VA) were cultured and grown on a swarm plate. 10 g of Difco Bacto tryptone, 5 g of yeast extract, 5 g of NaCl, and 6 g of Difco Bacto agar were dissolved into 1000 ml of de-ionized water to prepare 0.6% agar plates for swarming bacteria,²⁰ followed by autoclaving the solution and dividing into 100 ml sterile bottles. This solution was stored at room temperature and solidified and was reliquified using a microwave on the lowest power set-

^{a)}Electronic mail: mkim@coe.drexel.edu.

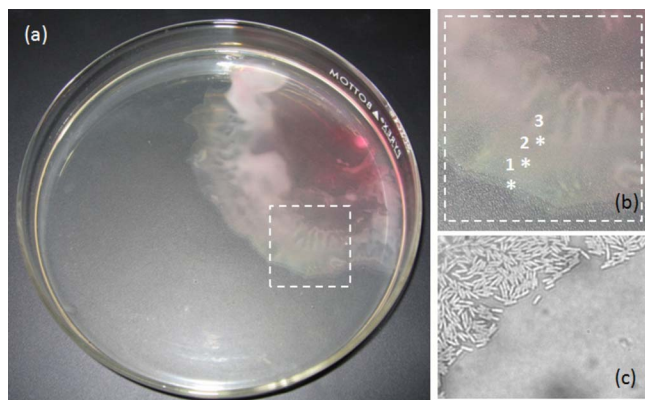


FIG. 1. (Color online) (a) Agar swarm plate of *S. marcescens* inoculated at upper right. (b) The swarm edge is marked by asterisk 1, and progressive videos of swarming were taken at 0.5 mm increments toward the inoculation site, as indicated by asterisks 2 and 3. (c) Individual swarmer cells can be identified along the swarm at 63 \times magnification.

ting. Before pouring individual agar plates, the 100 ml of prepared agar solution was mixed with 2 ml of 25% glucose solution. 1.5 ml of this new agar solution was pipetted into 35 mm Petri dishes. The dish was cooled to room temperature and allowed to resolidify. The swarm plate was inoculated on one edge with 2 μ l of *S. marcescens* saturated culture. Agar plates were incubated at 30–34 $^{\circ}$ C, and swarming began within 8–16 h. The inoculation site generally turned pink shortly after the swarming motion developed. The swarm progressed across the plate in waves that appeared as irregular concentric rings with the most active bacteria along the outermost edge of the swarm.

Consecutive images (15 frames/s) describing the minute motions of the bacteria swarming at 0.5 mm increments starting from the edge of the swarm, shown in Fig. 1, were captured and digitized using a phase-contrast microscope (AmScope) equipped with a 40 \times objective and a charge coupled device camera (Sony, model XC-75) and imported into MATLAB for analysis of the flow field.

Changes in velocity of the bacteria were found due to frame-to-frame velocity variations when all images were used. The 400 \times 400 pixel [86 \times 86 μ m², actual dimensions, Fig. 2(a)] investigation region was swarmed with thousands of bacteria. These cells varied in length from 5 to 10 μ m and

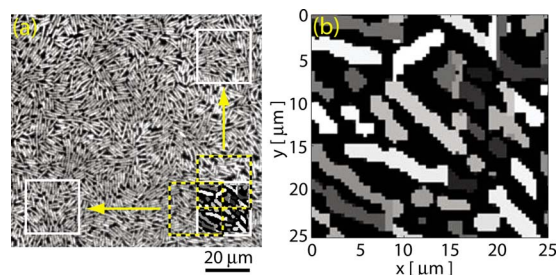


FIG. 2. (Color online) (a) Swarming *S. marcescens* on an agar plate. Instead of tracking each individual cell, local interrogation windows were defined to analyze the averaged velocities. Neighboring windows were overlapped by 50% and are described by the dashed squares. (b) Cell bodies were unable to be individually isolated and tracked due to close proximity.

are covered with numerous (10–100) petrichously or laterally situated flagella.²⁰

Ideally, every individual bacterium would be traced and analyzed for velocity field analysis. If this were possible, a typical particle tracking velocimetry scheme could be used for velocity calculations. However, as shown in Fig. 2(b), individual bacteria swarming in close proximity have overlapping or otherwise unclear boundaries due to close contact and inherent resolution limits of light microscopy. Also, the distance of the bacterial monolayer measured from the leading edge of the swarm to the development of a multilayer varied from 15 to 100 μ m along the swarm edge. To create a solution to these difficulties, small interrogation windows (20 \times 20 pixel, 4.3 \times 4.3 μ m²) for locally averaged velocity analysis were defined. It should be noted that this window only contains a total of five to ten swarming bacteria on average. As shown in Fig. 2(a), the interrogation windows were repeated with 10 pixel shifts (50% overlap) both in the horizontal (x) and vertical (y) directions over the entire investigation region. For the current study, the total number of interrogation windows is 1296 (36 \times 36 windows). Each interrogation window included several bacteria which were generally heading toward similar directions. Along the edges of these windows, only the fraction of the individual cell bodies present in the window was included for calculation. To investigate an averaged velocity to compensate for all bacterial motions involved in an interrogation window, two temporally consecutive (images at time t and $t+\Delta t$, $\Delta t = 1/15$ s in this study) but spatially identical interrogation windows were compared by shifting the latter interrogation window (at time $t+\Delta t$) by 1 pixel in every major or diagonal direction with respect to the center of the former interrogation window (time t). The minimum change in pixel intensity value was found by subtracting one window from the other and consequently obtaining the new center of the shifted interrogation window in the image at time t . This indicates that shifting with the bulk movement of a small group of bacteria generally caused the minimum difference. After one process of single-pixel shifting, the next shifting process started over with respect to the new center of the shifted interrogation window (still at time t) with the new interrogation window which is again temporally consecutive and spatially the same. This process of single-pixel shifting was performed in order of “top to bottom” and “left to right” and was repetitively performed ten times for every time interval for all interrogation windows over the entire investigation region and also for all 300 images. By shifting ten times for each window, a very precise measurement can be made for each velocity vector, but to ensure accuracy, the time interval Δt must be small enough so that temporally consecutive windows do not shift to a degree greater than the scale of the interrogation window itself.

To further investigate the patterns of the entire flow field generated by the collective motion of the swarming bacteria, the velocity field on the swarm was spatially correlated. The spatial correlation function offers an insight to the degree to which the swarming bacteria are coordinated in some direction for any given area of interest. The spatial correlation function is defined as

$$\Omega(|\vec{s}|) \equiv \frac{\langle \vec{V}(\vec{r}) \cdot \vec{V}(\vec{r} + \vec{s}) \rangle}{\langle \vec{V}(\vec{r}) \cdot \vec{V}(\vec{r}) \rangle},$$

where the angular brackets represent an ensemble average, \vec{V} is the averaged velocity for each interrogation window, \vec{r} is the position vector of the center of each window, and \vec{s} is the vector between the centers of two windows being interrogated. Once two velocity vectors are highly correlated with each other, i.e., “aligned” with an acute angle between two vectors, the inner product for the velocities yields a positively large value, while orthogonally oriented velocities yield zero and obtuse-angled vectors yield negative values. The correlation length can be determined by integrating Ω with respect to the in-between distance s .

Although cell culturing is performed with the same batches of nutrients and chemicals, swarms demonstrate noticeable variations. This is likely due to minute changes in the characteristics of the immediate surroundings of the bacteria such as variations in surface moisture, surface topography, or local nutrient content. Due to these inherent variations between different swarms and along the edges of a single swarm, multiple images and data sets were captured for an averaged analysis of swarm motility.

RESULTS AND DISCUSSION

The computed flow fields qualitatively matched the motion of the original image sequences upon visual inspection with the computed vectors superimposed on the original video. The velocity field of the swarming bacteria typically featured the combination of curvilinear translation and vortex modes. The bacteria formed several groups over the entire investigation region for a short time period, mostly translating along rather curved paths. They joined temporarily large streams but shortly after branched off in all directions and joined other streams, forming another translational stream or sometimes vortices. They repeated these patterns and the density of the bacteria in the investigated region appeared quite constant.

Figure 2(a) shows the active swarming behavior of the bacteria on an agar plate. The agar plate was swarmed with thousands of swarming *S. marcescens*. The bacteria formed a dense monolayer carpet on the agar plate. The overall appearance seems to be random, but upon close inspection, the cells reveal complex coordinated flow patterns composed of curvilinear motions and vortices.

Figure 3 shows the typical flow field of the investigated region and the arrows indicate the averaged magnitude and direction of the velocities for individual local interrogation windows. For the region within 1 mm from the edge, the bacteria on the agar plate seem to consist of many curved streams with average speed of $13.4 \mu\text{m/s}$ (maximum of $16.7 \mu\text{m/s}$) as shown in Fig. 4 and vortices rotating both clockwise and counterclockwise, normally $25\text{--}30 \mu\text{m}$ in diameter. The diameter of the vortices was four to five bacterium lengths based on the elongated cellular form ($6\text{--}7 \mu\text{m}$) on the swarm plate.²⁰ The vortices seem to be induced by several neighboring curved large streams. Some bacteria

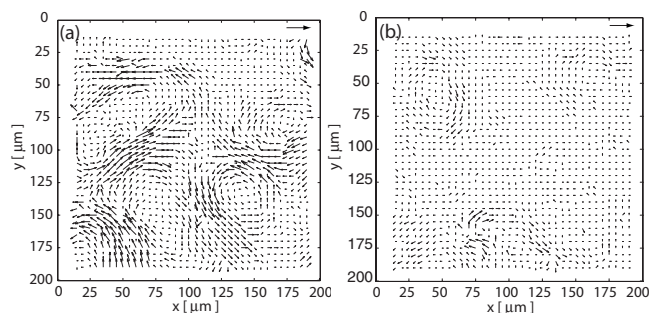


FIG. 3. Instantaneous bacterial swarming flow field (a) at the edge and (b) 4 mm from the swarm edge. The cells revealed complex flow patterns composed of curvilinear motions and vortices. The arrow (\rightarrow) denotes a speed of $35 \mu\text{m/s}$.

branched off from the main streams and joined other streams, but some formed vortices, which again merged into an adjacent stream or disappeared shortly.

There is a consistent increase in average velocity from the edge of the swarm to roughly 0.45 mm. At the edge of the swarm, individual bacteria are unable to move due to the semisolid, highly viscous nature of the agar. As the region of interest progresses further from the edge of the swarm, the bacteria move more freely due to the relative motility of the neighboring bacteria. An analogy can be made between the classic parabolic profile of viscous flow in a channel and the region between the edge of the swarm and 0.45 mm. It should also be considered that the bacteria secrete serrawettin, a surface active exolipid which wets the agar surface and enhances motility.²¹

As the region of interest passes 0.45 mm from the swarm edge, the motility decreases. This may be due to entanglement of flagella between adjacent cells as density increases. Also, typically between 1 and 4 mm from the edge, a multilayer wave of immotile bacteria consistently overcomes the swarm. There is no coordinated movement after this wave passes in the sense that the bacteria do not exhibit collective motion in the form of streams and vortices. However, there is still an extremely slow progression of cells toward the swarm edge. Keeping in mind that the cells in this region are as yet quite alive and continue to reproduce, this is most likely due to the forces of biomass production causing

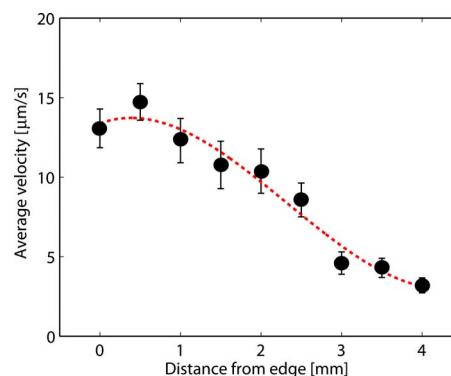


FIG. 4. (Color online) Average velocities at different locations from the swarm edge using multiple data sets. Due to strong vortices and translational motion, the near-edge regions have the largest average velocities.

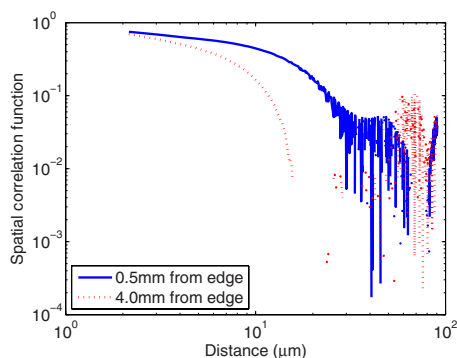


FIG. 5. (Color online) Normalized spatial correlations, $\Omega(|s|)$, as a function of the distance between individual interrogation windows over 0.5 and 4 mm investigation domains.

a form of plug flow of entangled, immotile cells. Due to the fact that Fig. 4 represents the average of several swarms, this appears as a linearly declining velocity when, in fact, for each individual swarm, velocity slowly decreases after 0.45 mm, then collective motion suddenly stops as the immotile wave is reached.

To further quantify the complex combination of the bacterial behaviors on the swarm plate, the spatial correlation function for the velocity field was obtained as a function of inter-interrogation window distance. Figure 5 shows the normalized correlation between the averaged velocities for each interrogation region. The figure indicates that immediately neighboring bacteria are headed in the same direction with less directional correlation as distance between bacteria increases. Where the values of the spatial correlation function fall below 0.1 (distances of 30–70 μm), the distance between flanks of both sides of the humps in the curves indicates the diameter of vortices.¹⁷ The average intervortex distance ranged from 30 to 35 μm .

The correlation length was determined by integrating the correlation function over distance (Fig. 6). The mean correlation length was $9.4 \pm 1.2 \mu\text{m}$ for the region within 1 mm from the edge. Bacteria very near the swarm edge (10–100 μm) are slowed due to viscous interactions with the set of bacteria which are directly situated on the leading

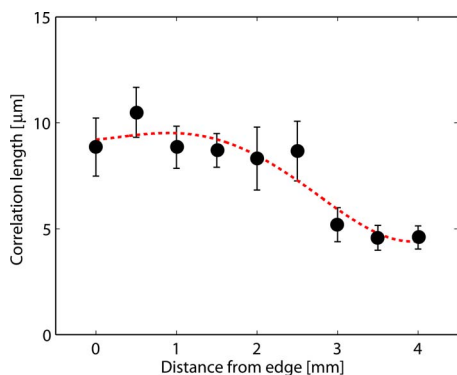


FIG. 6. (Color online) Correlation lengths at different locations averaged over multiple swarms. The higher activity within 1 mm from the swarm edge appears to affect the degree to which the swarming bacteria are coordinated in a given direction for a given area of interest.

edge of the swarm (0–10 μm from the swarm edge). These bacteria of the edge of the swarm are themselves unable to move and may remain in place for tens of seconds before being pushed by the swarm. However, bacteria at 0.5 mm are less restricted and thus able to attain greater correlation length. The maximum correlation occurs at roughly 0.9 mm. The slight increase from the edge to 0.5 mm is again likely due to the lack of influence of immotile bacteria at the swarm edge. The correlation length decreases past 0.9 mm from the edge due to flagellar entanglement, and the sudden drop around 3–4 mm can again be attributed to the inactive waves of entangled bacteria that follow the freely moving near-edge region.

This complex pattern is driven by surging bacterial crowds whose direction is not predictable. Sudden formations of helically directed surges generate large velocity gradients at a local region and replenish the stream with the local cells which then return into transient vortex domains.

The average velocities and spatial correlation lengths reveal that the swarm enables rapid population of semisolid surfaces. Bacteria with the greatest velocities and correlations are active along the edge. The consequence of this is that collectives of cells act as battering rams against the immotile bacteria along the swarm edge. This hammering motion pushes the otherwise immotile cells along the very edge of the swarm enabling wetting of the surface. The high momentum due to surging motion of several hundred or even thousand cells enables the swarm to rapidly proceed. The seemingly random nature of the surges averages across the edge of the swarm with several surges occurring within a minute near any given point along the edge. The cells decrease in motility and eventually stop moving completely in the region between 2 and 4 mm inside the swarm from the edge. It is hypothesized that the cells in the swarm interior are not responsible for rapid population and progression of the swarm and thus motility in the form of streams and vortices is not required.

CONCLUSION

In this study, we used a non labeled cell tracking algorithm for characterizing the flagellated bacterial swarming motion on a soft agar plate without fluorescence labeling or help of microspheres as tracers. This method calculates average velocities for local regions regularly arranged over the entire flow field composed mostly of curvilinear bacterial stream and vortices.

The tracking method was further applied to study the motility of swarming bacteria as a function of distance from the swarm edge. It was discovered that the average velocities were not highest at the very edge of the swarm but actually reached the maxima in the areas roughly 450 μm from the edge. The maximum for the correlation length was also found to occur roughly 900 μm from the swarm edge. This indicates that the bacterial flows align for the longest distances in this region. The data suggest that the high velocity, surging motions of the swarming cells cause a viscous push to the swarm edge and enable rapid population of the surface.

ACKNOWLEDGMENTS

The authors acknowledge the invaluable contributions of Svetlana Rojevskaya, Linda Turner, and Howard Berg for access to their bacteria strains, expertise, and experience in culturing and handling *S. marcescens*. Special thanks go to Kenny Breuer for his useful conversations. This work was supported by Drexel start-up funds (M.J.K.) and in part by NSF Contract No. DGE-0538476 (E.B.S.).

- ¹H. C. Berg and R. A. Anderson, "Bacteria swim by rotating their flagellar filaments," *Nature (London)* **245**, 380 (1973).
- ²J. Henriksen, "Bacterial surface translocation: A survey and a classification," *Bacteriol. Rev.* **36**, 478 (1972).
- ³H. C. Berg, "The rotary motor of bacterial flagella," *Annu. Rev. Biochem.* **72**, 19 (2003).
- ⁴M. Matsushita, in *Bacteria as Multicellular Organisms*, edited by J. A. Shapiro and M. Dworkin (Oxford University Press, New York, 1997).
- ⁵N. H. Mendelson, A. Bourque, K. Wilkening, K. R. Anderson, and J. C. Watkins, "Organized cell swimming motions in *Bacillus subtilis* colonies: Patterns of short-lived whirls and jets," *J. Bacteriol.* **181**, 600 (1999).
- ⁶E. Ben-Jacob, I. Cohen, A. Czirok, T. Vicsek, and D. L. Gutnick, "Chemomodulation of cellular movement, collective formation of vortices by swarming bacteria, and colonial development," *Physica A* **238**, 181 (1997).
- ⁷C. Dombrowski, L. Cisneros, S. Chatkaew, R. E. Goldstein, and J. O. Kessler, "Self-concentration and large-scale coherence in bacterial dynamics," *Phys. Rev. Lett.* **93**, 098103 (2004).
- ⁸J. P. Hernandez-Ortiz, C. G. Stolz, and M. D. Graham, "Transport and collective dynamics in suspensions of confined swimming particles," *Phys. Rev. Lett.* **95**, 204501 (2005).
- ⁹A. Sokolov, I. S. Aranson, J. O. Kessler, and R. E. Goldstein, "Concentration dependence of the collective dynamics of swimming bacteria," *Phys. Rev. Lett.* **98**, 158102 (2007).
- ¹⁰V. Narayan, S. Ramaswamy, and N. Menon, "Long-lived giant number fluctuations in a swarming granular nematic," *Science* **317**, 105 (2007).
- ¹¹J. Starruss, F. Peruani, M. Bar, and A. Deutsch, in *Mathematical Modeling of Biological Systems*, edited by A. Deutsch, L. Bruschi, H. Byrne, G. de Vries, and H. Herzel (Birkhauser, Boston, 2007).
- ¹²L. H. Cisneros, R. Cortez, C. Dombrowski, R. E. Goldstein, and J. O. Kessler, "Fluid dynamics of self-propelled microorganisms, from individuals to concentrated populations," *Exp. Fluids* **43**, 737 (2007).
- ¹³M. J. Kim and K. S. Breuer, "Microfluidic pump powered by self-organizing bacteria," *Small* **4**, 111 (2008).
- ¹⁴E. Steger, C.-B. Kim, J. Patel, S. Bith, C. Naik, L. Reber, and M. J. Kim, "Control of microfabricated structures powered by flagellated bacteria using phototaxis," *Appl. Phys. Lett.* **90**, 263901 (2007).
- ¹⁵S. Martel, C. C. Tremblay, S. Ngakeng, and G. Langlois, "Controlled manipulation and actuation of micro-objects with magnetotactic bacteria," *Appl. Phys. Lett.* **89**, 233904 (2006).
- ¹⁶B. Behkem and M. Sitti, "Bacterial flagella-based propulsion on/off motion control of microscale objects," *Appl. Phys. Lett.* **90**, 023902 (2007).
- ¹⁷N. Darnton, L. Turner, K. S. Breuer, and H. C. Berg, "Moving fluid with bacterial carpets," *Biophys. J.* **86**, 1863 (2004).
- ¹⁸H. C. Berg and D. A. Brown, "Chemotaxis in *Escherichia coli* analysed by three-dimensional tracking," *Nature (London)* **239**, 500 (1972).
- ¹⁹M. J. Kim and K. S. Breuer, "Controlled mixing in microfluidic systems using bacterial chemotaxis," *Anal. Chem.* **79**, 955 (2007).
- ²⁰L. Alberti and R. M. Harshey, "Differentiation of *Serratia marcescens* 274 into swimmer and swarmer cells," *J. Bacteriol.* **172**, 4322 (1990).
- ²¹H. Li, T. Tanikawa, Y. Sato, Y. Nakagawa, and T. Matsuyama, "*Serratia marcescens* gene required for surfactant serrawetting W1 production encodes putative aminolipid synthetase belonging to nonribosomal peptide synthetase family," *Microbiol. Immunol.* **49**, 303 (2005).